Recent Progress in Neutron-Antineutron Oscillation Theory

Michael Wagman (UW/INT)

Quark Confinement and the Hadron Spectrum XII

with Michael Buchoff, Enrico Rinaldi,
Chris Schroeder, and Joe Wasem (LLNL),
and Sergey Syritsyn (Jefferson Lab/Stony Brook)

Neutron-Antineutron Oscillations

$n\overline{n}$ violates fundamental symmetries of baryon number and $B - L$, sensitive to different physics than proton decay

Testable signature of possible BSM baryogenesis mechanisms explaining matter-antimatter asymmetry

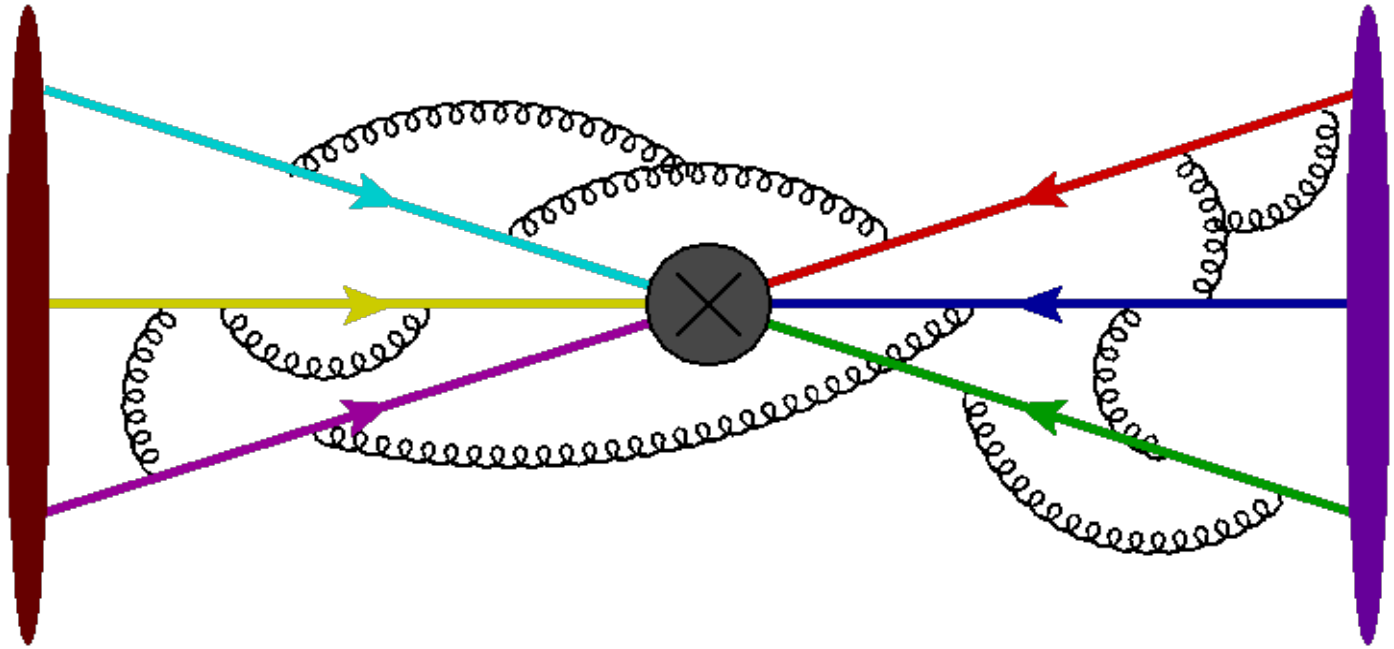

Neutron-Antineutron Phenomenology

Similarities to kaon, neutrino oscillations

$$P_{n\bar{n}}(t) = \sin^2(t/\tau_{n\bar{n}})e^{-\Gamma_n t} \qquad \frac{1}{\tau_{n\bar{n}}} = < \bar{n}|H_{n\bar{n}}|n >$$

Magnetic fields, nuclear interactions modify transition rate

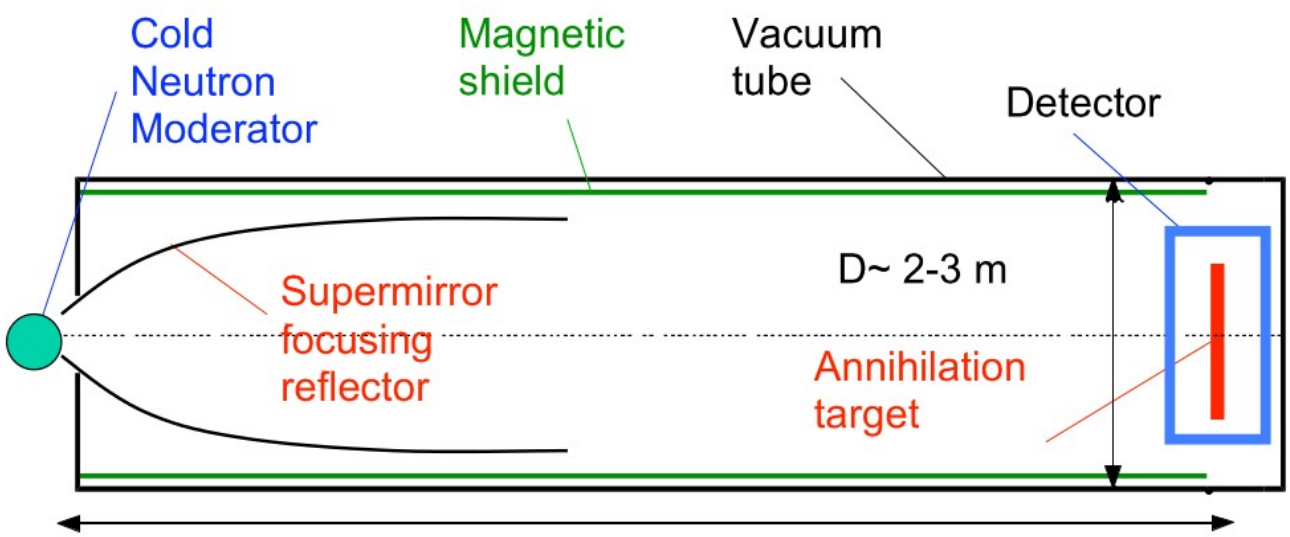

Mohapatra (2009)

Experimental Constraints

ILL: $\tau_{n\bar{n}} > 2.7$ years

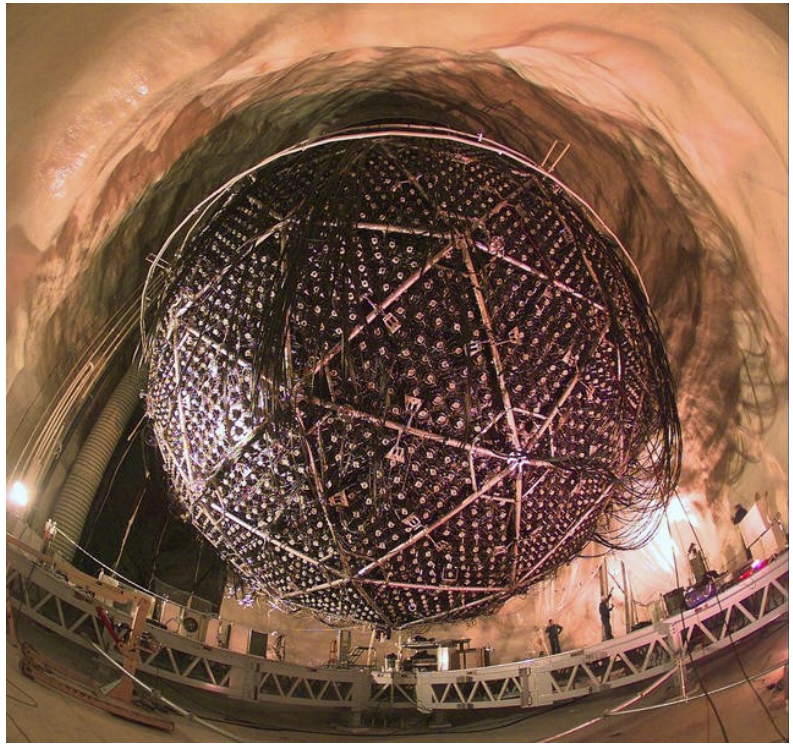

SNO: $\tau_{n\bar{n}} > 5.7$ years (preliminary)

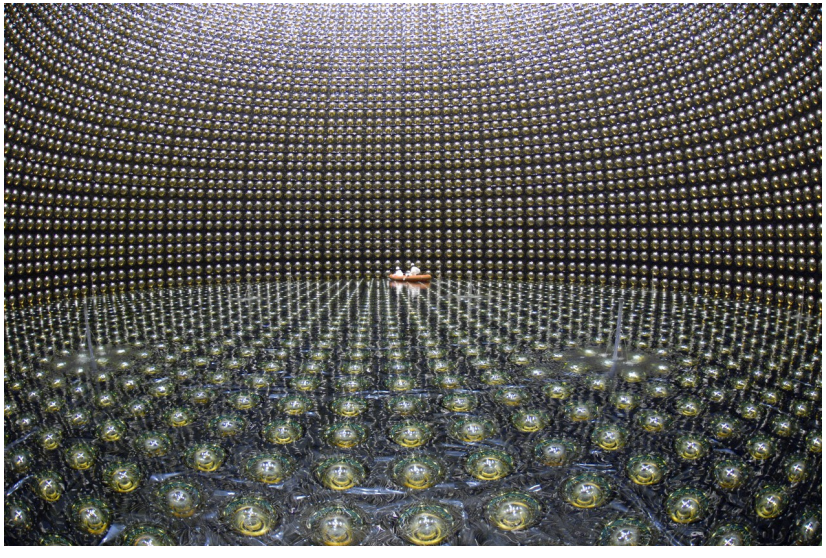

Super K: $\tau_{n\bar{n}} > 11$ years

Experimental Outlook

European Spallation Source could have 1000 times ILL sensitivity, probe 30 times higher $\tau_{n\bar{n}}$ within next decade

Neutron-Antineutron Theory: The Standard Model and Beyond

Theory must make robust predictions for $\tau_{n\overline{n}}$ to reliably interpret the constraints from these experiments

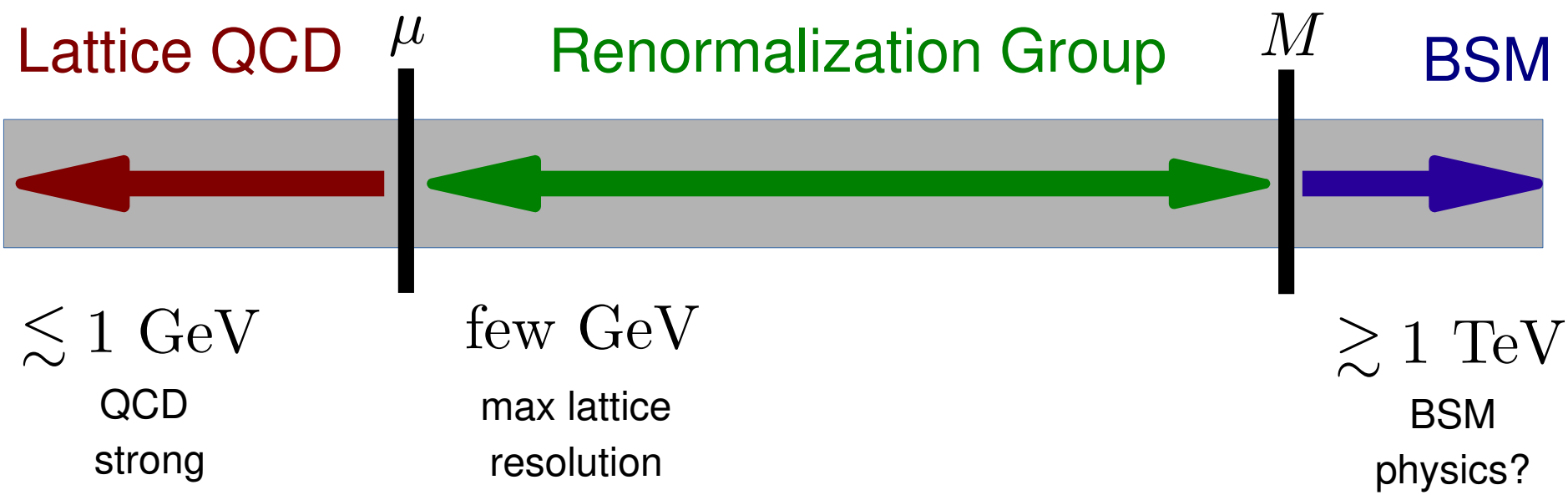

Baryogenesis

Baryon asymmetry and $n\overline{n}$ produced by same interactions in several BSM theories

Post-sphaleron baryogenesis in e.g. left-right symmetric theories predicts there is a theoretical upper bound on $\tau_{n\overline{n}}$

Babu, Dev, Fortes, and Mohapatra (2013)

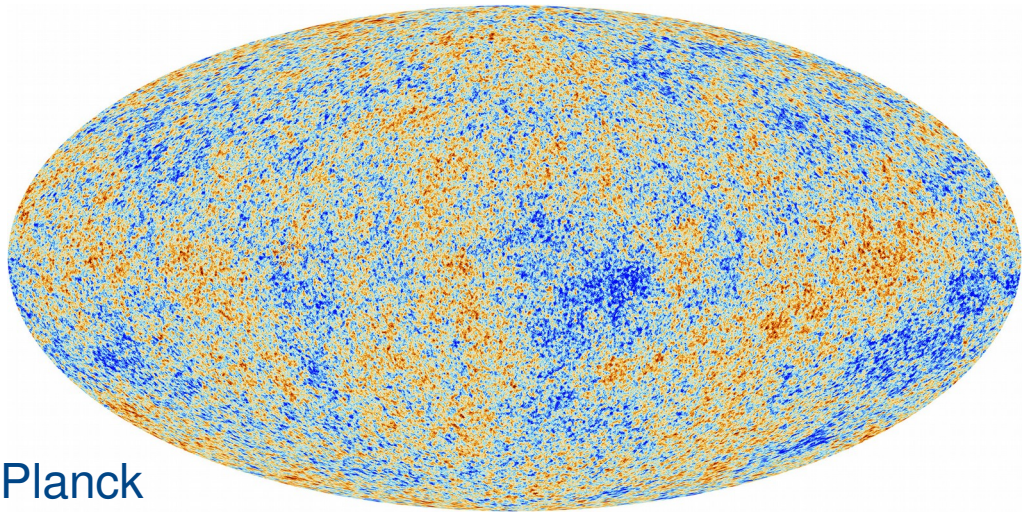

Planck

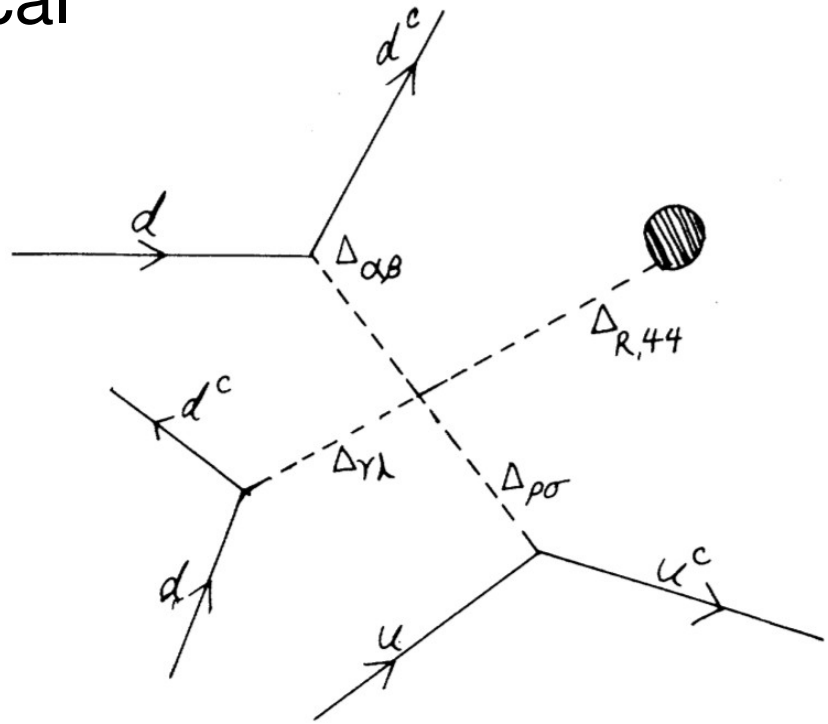

Mohapatra and Marshak (1980)

Six-Quark Operators

SM effective theory describes $n\overline{n}$ with six-quark operators

$$\mathcal{H}_{n\bar{n}} = \sum_I C_I^{\overline{\mathrm{MS}}}(M) Q_I^{\overline{\mathrm{MS}}}(M) \qquad Q_I \sim uuddd d$$

BSM theories predict coefficients at high scales

Early estimates of six-quark matrix elements in bag model Rao and Shrock (1984)

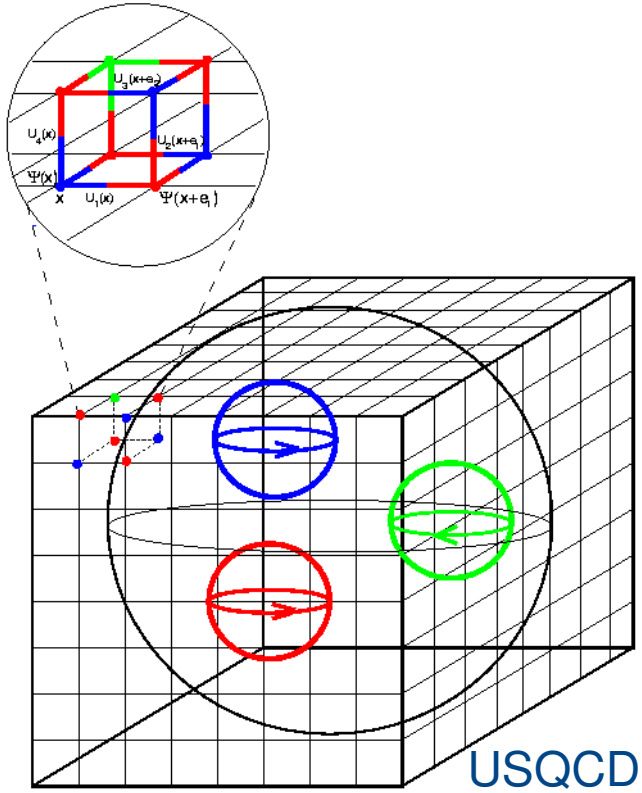

Lattice QCD needed for reliable connection between BSM predictions and experimental constraints on $\tau_{n\overline{n}}$

$$\psi = \begin{pmatrix} u \\ d \end{pmatrix}$$

Chiral Operator Basis

$$Q_1 = (\psi C P_R i\tau^2 \psi)(\psi C P_R i\tau^2 \psi)(\psi C P_R i\tau^2 \tau^+ \psi) T^{AAS} = \mathcal{D}_R \mathcal{D}_R \mathcal{D}_R^+ T^{AAS}$$

Chiral Basis	Fixed-Flavor Basis	Chiral Tensor Structure	Chiral Irrep
Q_1	$\mathcal{O}^3_{RRR}$	$\mathcal{D}_R \mathcal{D}_R \mathcal{D}_R^+ T^{AAS}$	$(\mathbf{1}_L, \mathbf{3}_R)$
Q_2	$\mathcal{O}^3_{LRR}$	$\mathcal{D}_L \mathcal{D}_R \mathcal{D}_R^+ T^{AAS}$	$(\mathbf{1}_L, \mathbf{3}_R)$
Q_3	$\mathcal{O}^3_{LLR}$	$\mathcal{D}_L \mathcal{D}_L \mathcal{D}_R^+ T^{AAS}$	$(\mathbf{1}_L, \mathbf{3}_R)$
Q_4	$4/5\ \mathcal{O}^2_{RRR} + 1/5\ \mathcal{O}^1_{RRR}$	$\mathcal{D}_R^{33+} T^{SSS}$	$(\mathbf{1}_L, \mathbf{7}_R)$
Q_5	$\mathcal{O}^1_{RLL}$	$\mathcal{D}_R^- \mathcal{D}_L^{++} T^{SSS}$	$(\mathbf{5}_L, \mathbf{3}_R)$
Q_6	$\mathcal{O}^2_{RLL}$	$\mathcal{D}_R^3 \mathcal{D}_L^{3+} T^{SSS}$	$(\mathbf{5}_L, \mathbf{3}_R)$
Q_7	$2/3\ \mathcal{O}^2_{LLR} + 1/3\ \mathcal{O}^1_{LLR}$	$\mathcal{D}_R^+ \mathcal{D}_L^{33} T^{SSS}$	$(\mathbf{5}_L, \mathbf{3}_R)$
$\widetilde{Q}_1$	$1/3\ \mathcal{O}^2_{RRR} - 1/3\ \mathcal{O}^1_{RRR}$	$\mathcal{D}_R \mathcal{D}_R \mathcal{D}_R^+ T^{SSS}$	$(\mathbf{1}_L, \mathbf{3}_R)$
$\widetilde{Q}_3$	$1/3\ \mathcal{O}^2_{LLR} - 1/3\ \mathcal{O}^1_{LLR}$	$\mathcal{D}_L \mathcal{D}_L \mathcal{D}_R^+ T^{SSS}$	$(\mathbf{1}_L, \mathbf{3}_R)$

Isospin 3 → Q_4

Not SM gauge invariant → Q_5, Q_6, Q_7

Redundant in $D = 4$ → $\widetilde{Q}_1$, $\widetilde{Q}_3$

Chiral symmetry provides a basis with no operator mixing

Tiburzi (unpublished)

Regularization-Independent Renormalization

RI-MOM scheme: hold vertex functions Λ_I fixed to tree-level values at chosen reference scale μ (momentum subtraction)

Martinelli et al (1995)

$\mathcal{P}_I$ projects contribution from tree-level $\Lambda_I^{(0)}$ → $[\mathcal{P}_I \Lambda_J(\mu)] = \delta_{IJ}$

Vertex function should preserve chiral symmetry

$$[\Lambda_I]^{\alpha\beta\gamma\delta\eta\zeta}_{ijklmn}(p) = \frac{1}{5}\left\langle Q_I(0)\,\bar{u}^\alpha_i(p)\bar{u}^\beta_j(p)\bar{d}^\gamma_k(p)\bar{d}^\delta_l(-p)\bar{d}^\eta_m(-p)\bar{d}^\zeta_n(-p)\right\rangle\Big|_{amp}$$
$$+\frac{3}{5}\left\langle Q_I(0)\,\bar{u}^\alpha_i(p)\bar{u}^\beta_j(-p)\bar{d}^\gamma_k(p)\bar{d}^\delta_l(p)\bar{d}^\eta_m(-p)\bar{d}^\zeta_n(-p)\right\rangle\Big|_{amp}$$
$$+\frac{1}{5}\left\langle Q_I(0)\,\bar{u}^\alpha_i(-p)\bar{u}^\beta_j(-p)\bar{d}^\gamma_k(p)\bar{d}^\delta_l(p)\bar{d}^\eta_m(p)\bar{d}^\zeta_n(-p)\right\rangle\Big|_{amp}$$

Syritsyn (2015)

Perturbative Renormalization

$$\mathcal{H}_{n\bar{n}} = \sum_I C_I^{\overline{\rm MS}}(M) Q_I^{\overline{\rm MS}}(M) = \sum_I C_I^{\overline{\rm MS}}(M) U_I(M,\mu) Q_I^{\rm RI}(\mu)$$

One-loop running: Caswell, Milutinovic, and Senjanovic (1983)

$$U_I(M,\mu) = \left(\frac{\alpha_s(\mu)}{\alpha_s(M)}\right)^{-\gamma_I^{(0)}/2\beta_0} \left[1 - r_I^{(0)} \frac{\alpha_s(\mu)}{4\pi} + \left(\frac{\beta_1 \gamma_I^{(0)}}{2\beta_0^2} - \frac{\gamma_I^{(1)}}{2\beta_0}\right) \frac{\alpha_s(\mu) - \alpha_s(M)}{4\pi} + O(\alpha_s(\mu)^2)\right]$$

One-loop matching
Buchoff, MW (2015)

Two-loop running,
needed for $\alpha_s(\mu)$ accuracy
Buchoff, MW (2015)

Negligible

One-Loop Matching

15 one-loop diagrams in 3 topologies

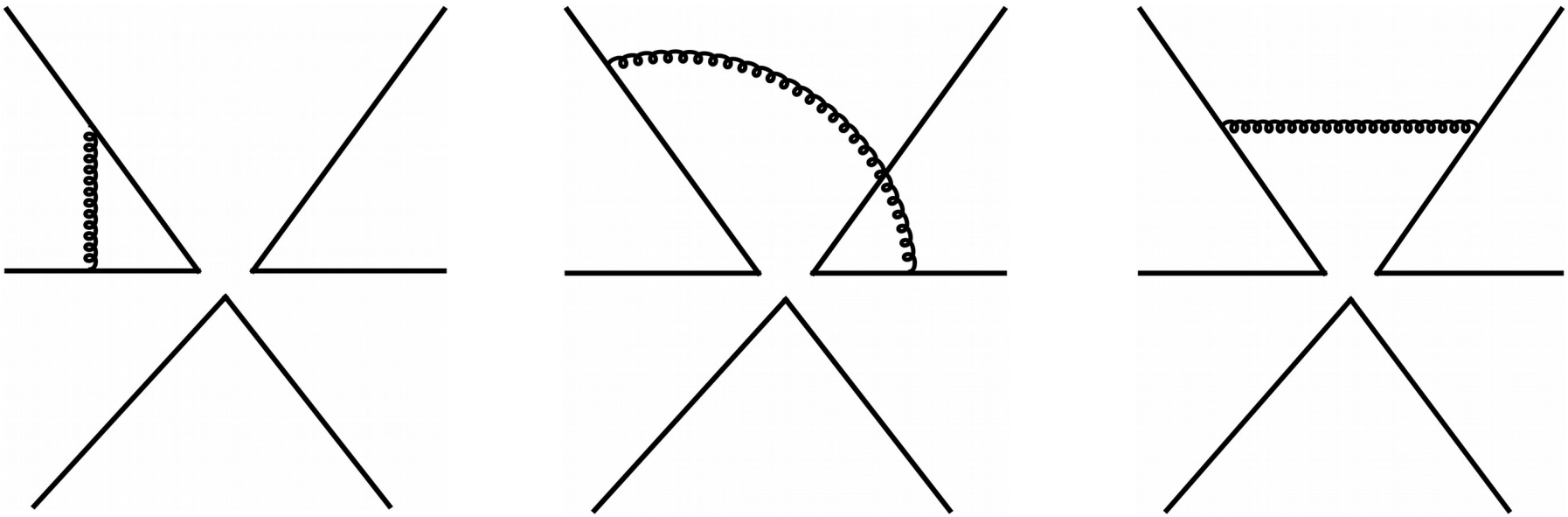

Same topologies appear in four-quark weak matrix elements and proton decay

Two-Loop Running

350 two-loop diagrams. Evanescent operators introduce complications

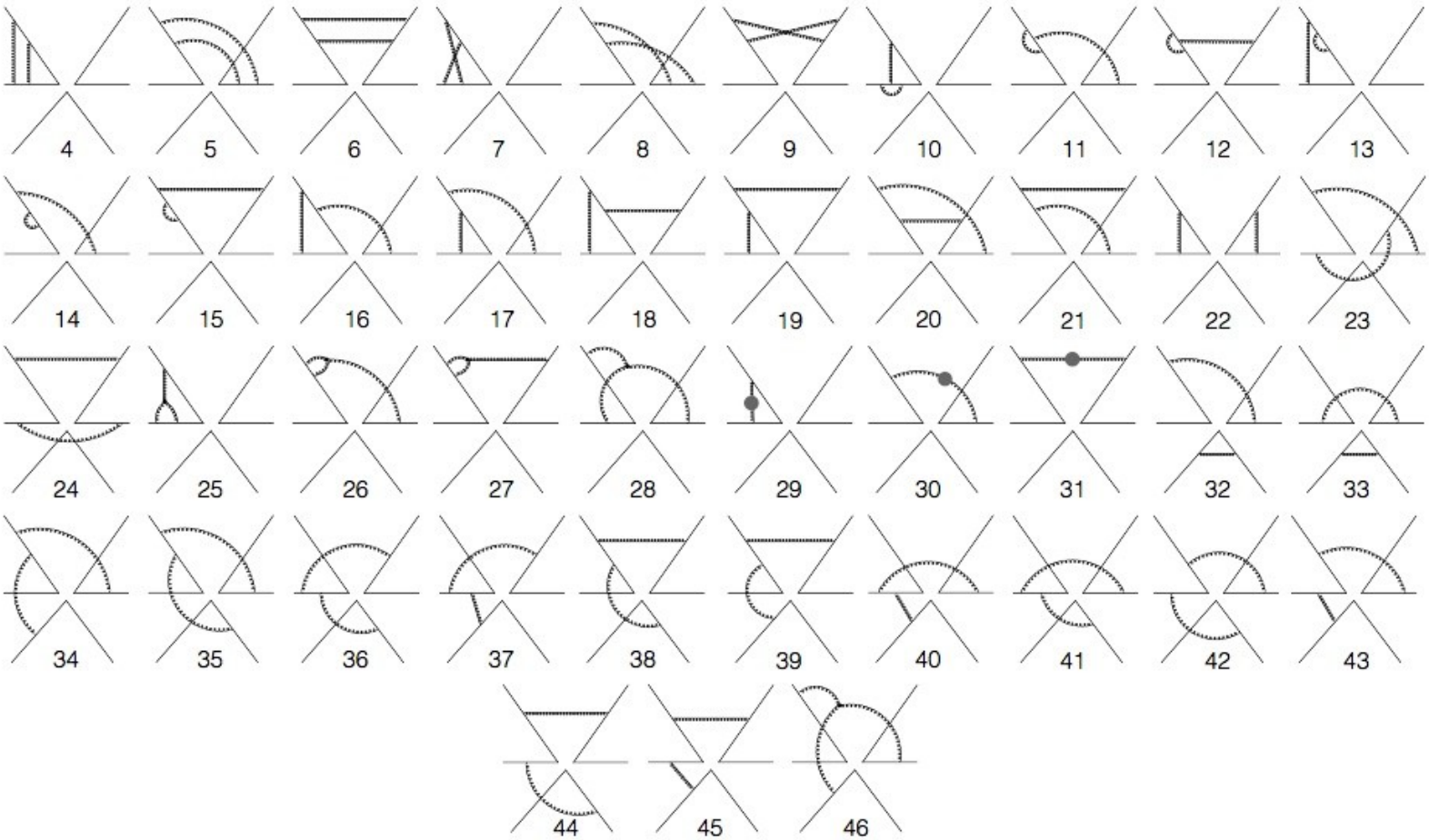

Includes all diagram topologies needed for two-loop running of any operator built from spin singlet diquarks

Perturbative Renormalization

Two-loop corrections $< 26\%$ at $\mu = 2\ \mathrm{GeV}$, perturbative matching under control

Operator renormalization effects significant

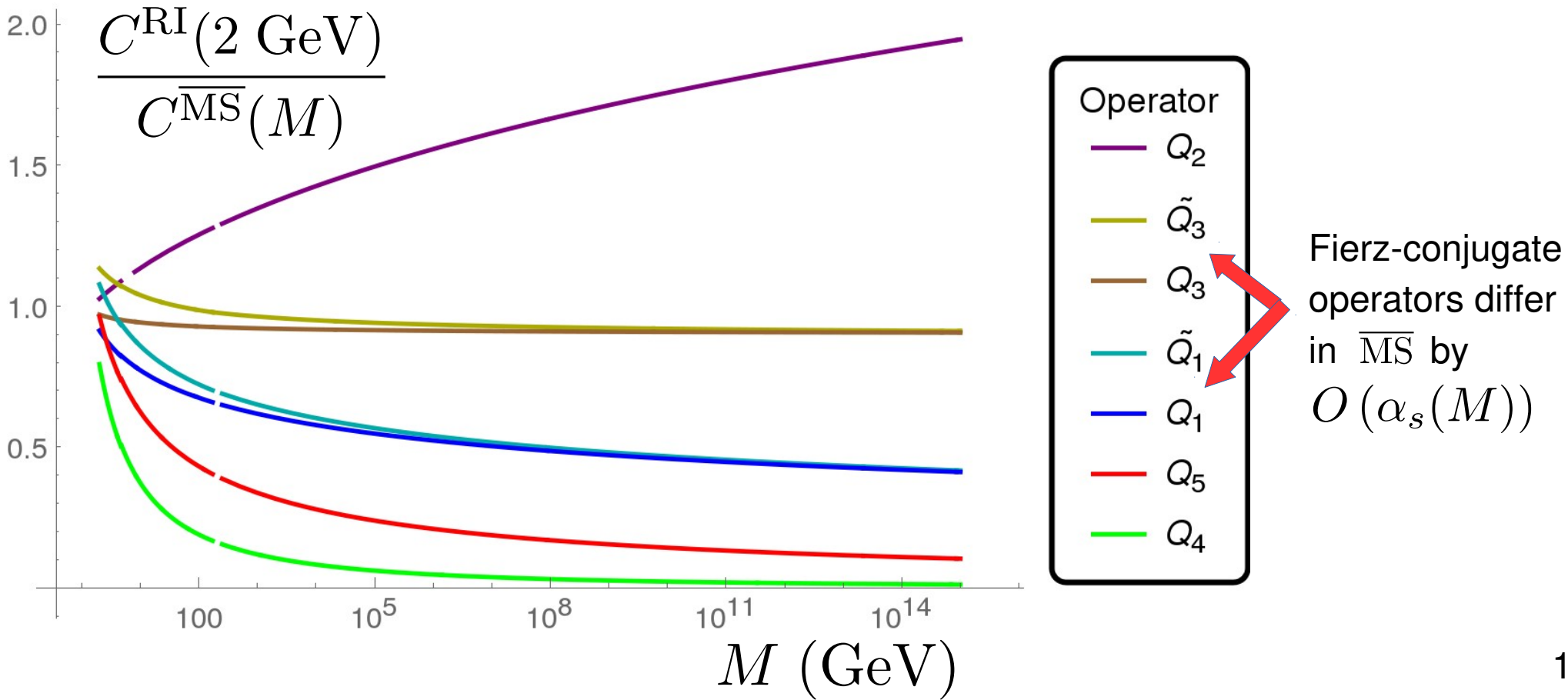

Non-Perturbative Renormalization

NPR complete, lattice artifacts small for most important operations

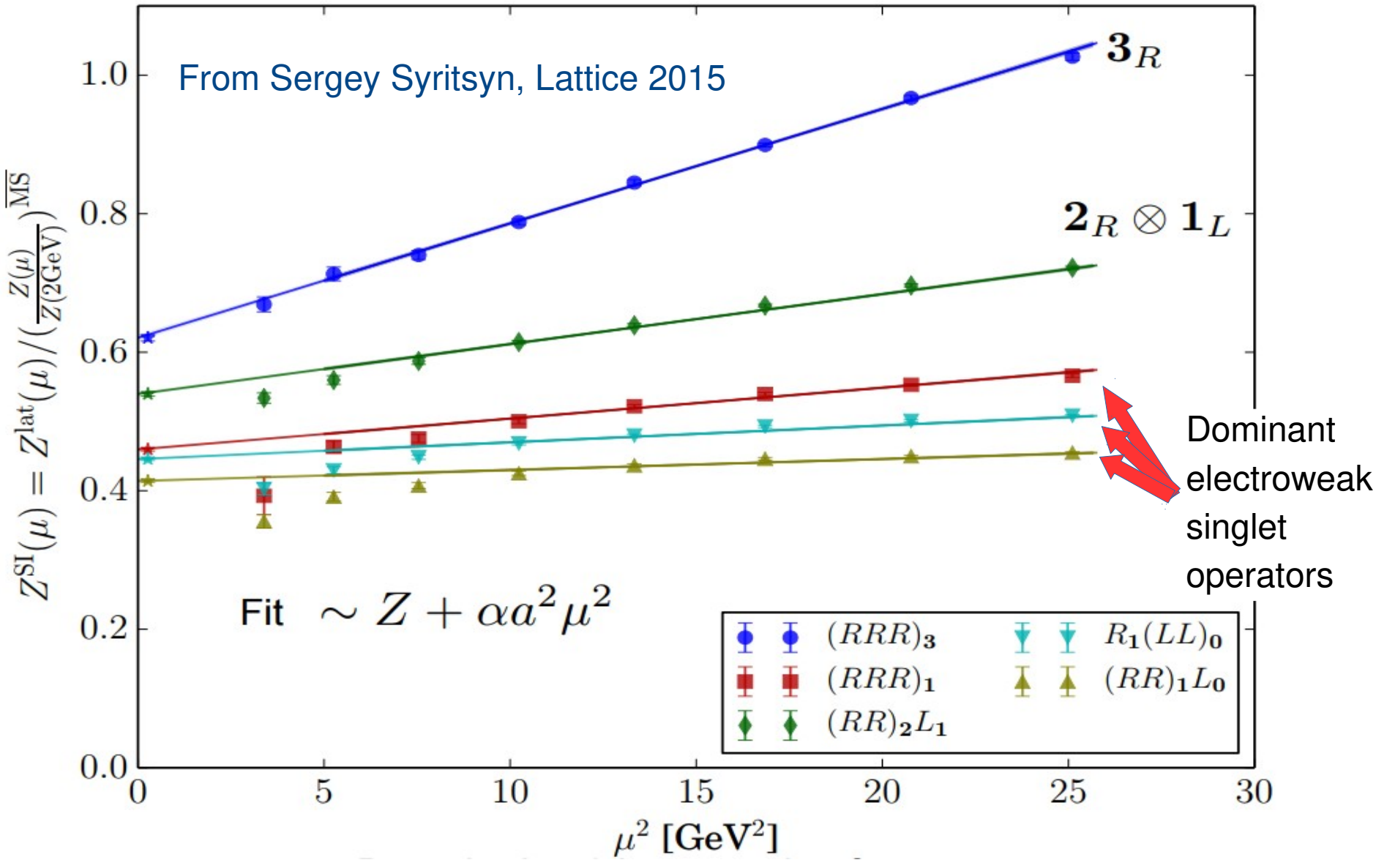

Lattice QCD Matrix Elements

LQCD matrix elements calculated from ratios of three-point to two-point correlation functions at large Euclidean time separations

$$< N_{\uparrow}^{(+)}(t_2) Q_I(0) N_{\downarrow}^{(-)}(-t_1) > \rightarrow \; Z_n Z_{\overline{n}} e^{-M_n(t_1+t_2)} < n|Q_I|\overline{n} >$$

Operator insertions at all time separations calculable from single point-to-all propagator

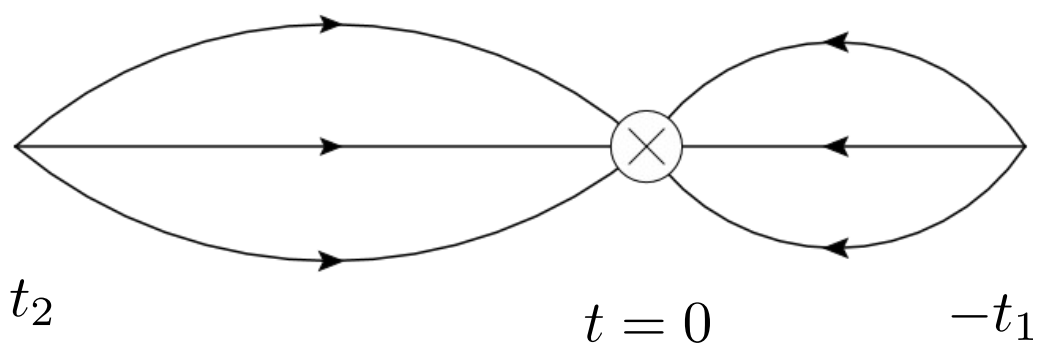

No disconnected diagrams

Exploratory LQCD Studies

Exploratory anisotropic Wilson calculation:

Buchoff, Schroeder, Wasem (2012)

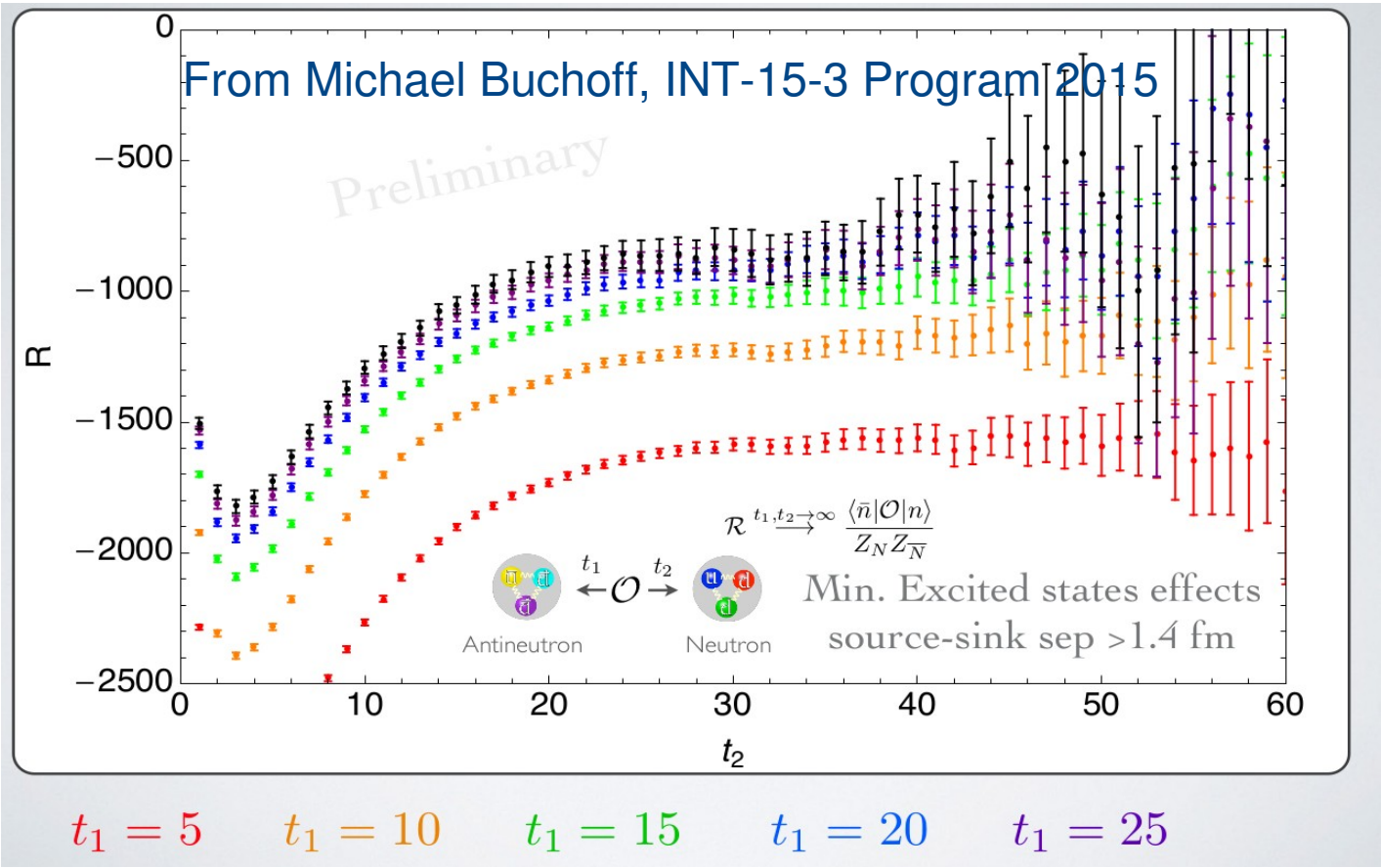

$a \sim 0.125$ fm $\quad m_\pi \sim 390$ Mev $\quad V = 20^3 \times 256$

Physical Point LQCD

Domain wall fermion calculation with RBC/UKQCD configurations

Syritsyn, Buchoff, Schroeder, Wasem (2015)

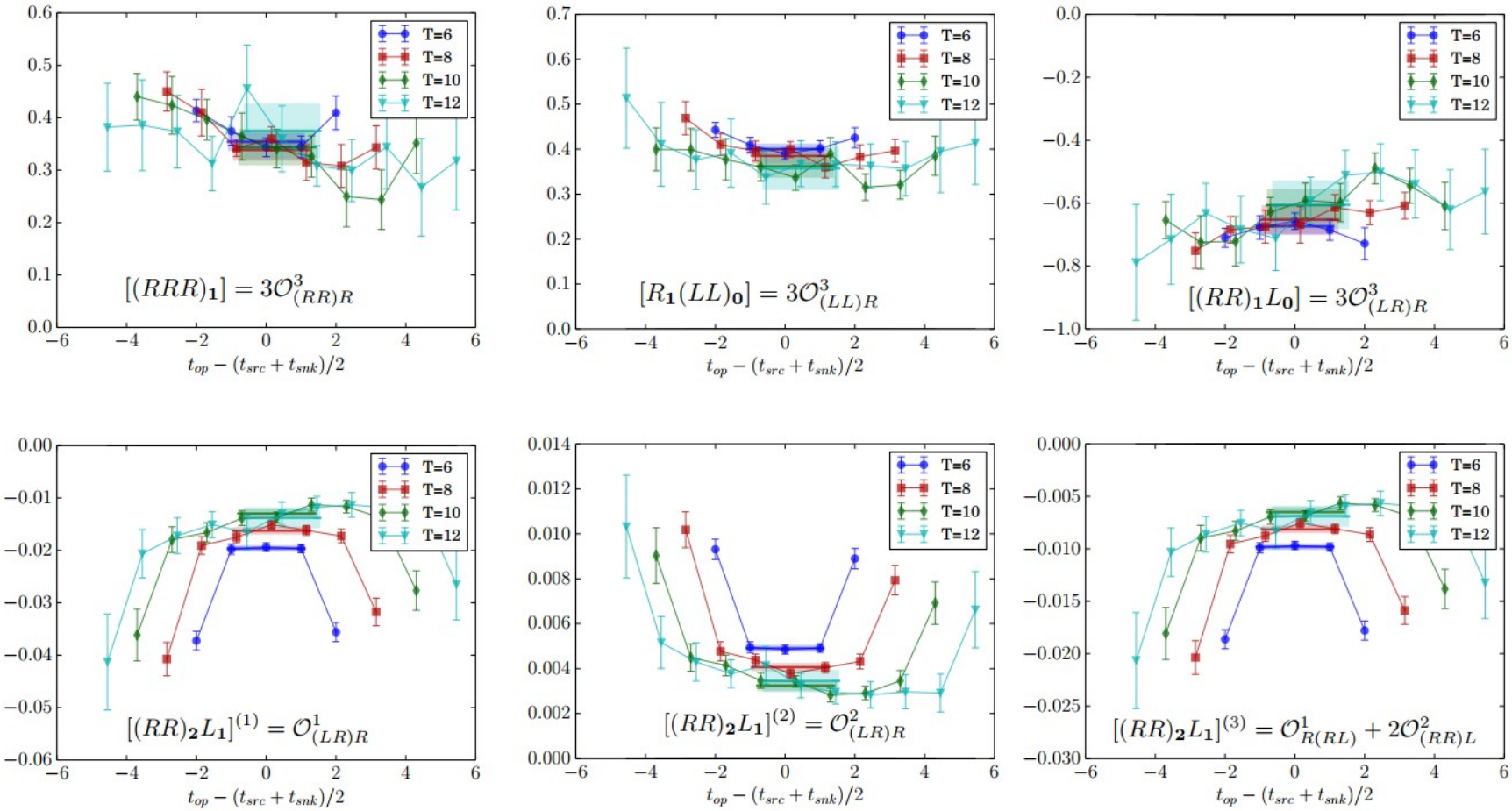

From Sergey Syritsyn, Lattice 2015

$a \sim 0.123$ fm $\quad m_\pi \sim 140$ Mev $\quad V = 48^3 \times 96$

Physical Point LQCD Results

	$Z(\text{lat} \to \overline{MS})$	$\mathcal{O}^{\overline{MS}(2\text{ GeV})}[10^{-5}\text{GeV}^6]$	Bag "A"	$\frac{\text{LQCD}}{\text{Bag "A"}}$	Bag "B"	$\frac{\text{LQCD}}{\text{Bag "B"}}$
$[(RRR)_3]$	0.62(12)	0	0	–	0	–
$[(RRR)_1]$	0.454(33)	45.4(5.6)	8.190	5.5	6.660	6.8
$[R_1(LL)_0]$	0.435(26)	44.0(4.1)	7.230	6.1	6.090	7.2
$[(RR)_1L_0]$	0.396(31)	-66.6(7.7)	-9.540	7.0	-8.160	8.1
$[(RR)_2L_1]^{(1)}$	0.537(52)	-2.12(26)	1.260	-1.7	-0.666	3.2
$[(RR)_2L_1]^{(2)}$	0.537(52)	0.531(64)	-0.314	-1.7	0.167	3.2
$[(RR)_2L_1]^{(3)}$	0.537(52)	-1.06(13)	0.630	-1.7	-0.330	3.2

Syritsyn, Buchoff, Schroeder, Wasem (2015)

Preliminary physical point results presented at Lattice 2015, final stages of the calculation underway with results to appear soon

Buchoff, Rinaldi, Schroeder, Syritsyn, MW, Wasem – *in prepartion*

Phenomenological Applications

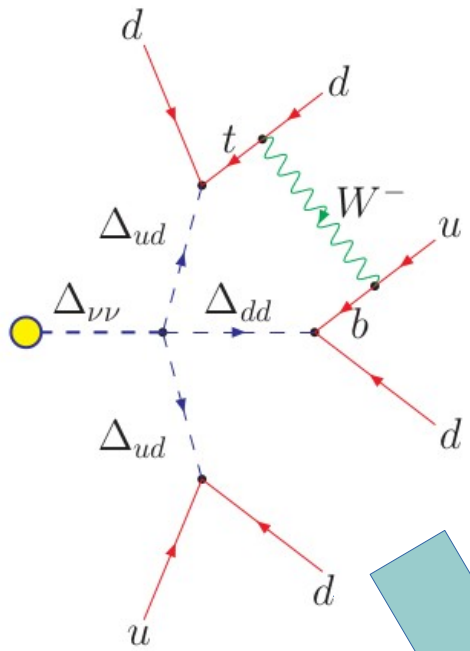

Babu et al (2013)

	$Z(\text{lat} \to \overline{MS})$	$\mathcal{O}^{\overline{MS}(2\,\text{GeV})}[10^{-5}\text{GeV}^6]$	Bag "A"	$\frac{\text{LQCD}}{\text{Bag "A"}}$	Bag "B"	$\frac{\text{LQCD}}{\text{Bag "B"}}$
$[(RRR)_3]$	0.62(12)	0	0	–	0	–
$[(RRR)_1]$	0.454(33)	45.4(5.6)	8.190	5.5	6.660	6.8
$[R_1(LL)_0]$	0.435(26)	44.0(4.1)	7.230	6.1	6.090	7.2
$[(RR)_1L_0]$	0.396(31)	-66.6(7.7)	-9.540	7.0	-8.160	8.1
$[(RR)_2L_1]^{(1)}$	0.537(52)	-2.12(26)	1.260	-1.7	-0.666	3.2
$[(RR)_2L_1]^{(2)}$	0.537(52)	0.531(64)	-0.314	-1.7	0.167	3.2
$[(RR)_2L_1]^{(3)}$	0.537(52)	-1.06(13)	0.630	-1.7	-0.330	3.2

Syritsyn, Buchoff, Schroeder, Wasem (2015)

$$\tau_{n\bar{n}}^{ILL} \geq 0.86 \times 10^8 \text{ s}$$

$$\tau_{n\bar{n}}^{ESS} \sim 2.7 \times 10^9 \text{ s}$$

$$\tau_{n\bar{n}}^{224,PSB} \leq (1.5 \pm 0.2) \times 10^{10} \text{ s}$$

Phenomenological studies needed to determine constraints of proposed ESS experiments on all BSM models of interest, e.g. Calibbi, et al (2016) for $\not{R}$ SUSY + bag model predictions

Summary

Low-energy $\mathrm{n\bar{n}}$ Hamiltonian relatively simple

– Three electroweak singlet operators in isospin limit, distinct chiral irreps

Experimental reach higher than expectated

– QCD matrix elements 5-10 times larger than bag model estimates for electroweak singlet operators

Operator color-flavor structure matters

– Different sign anomalous dimensions among electroweak singlet operators

– Non-singlet matrix elements 1-2 orders of magnitude smaller than singlets

Concrete BSM predictions including final LQCD results essential to assess reach of proposed ESS experiments

– Can post-sphaleron baryogenesis models be definitively tested at ESS?

Outlook

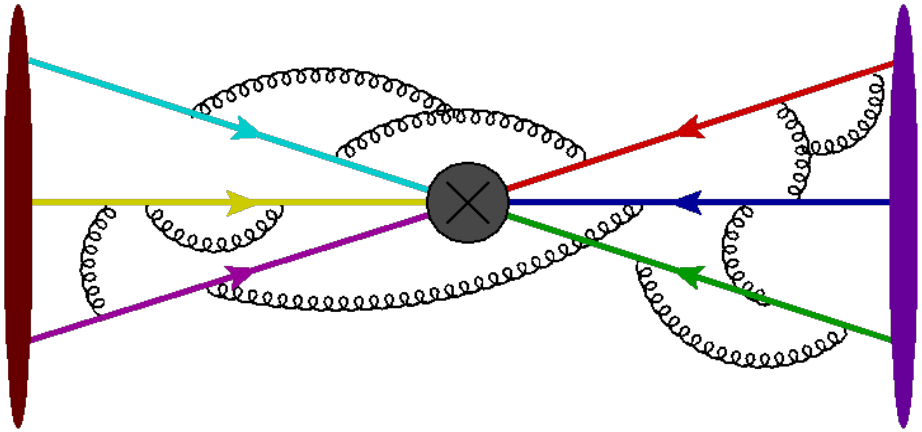

Exciting days ahead for $n\overline{n}$, stay tuned!